iScience

CellPress
OPEN ACCESS

Article

GINS1 promotes the proliferation and migration of glioma cells through USP15-mediated deubiquitination of TOP2A

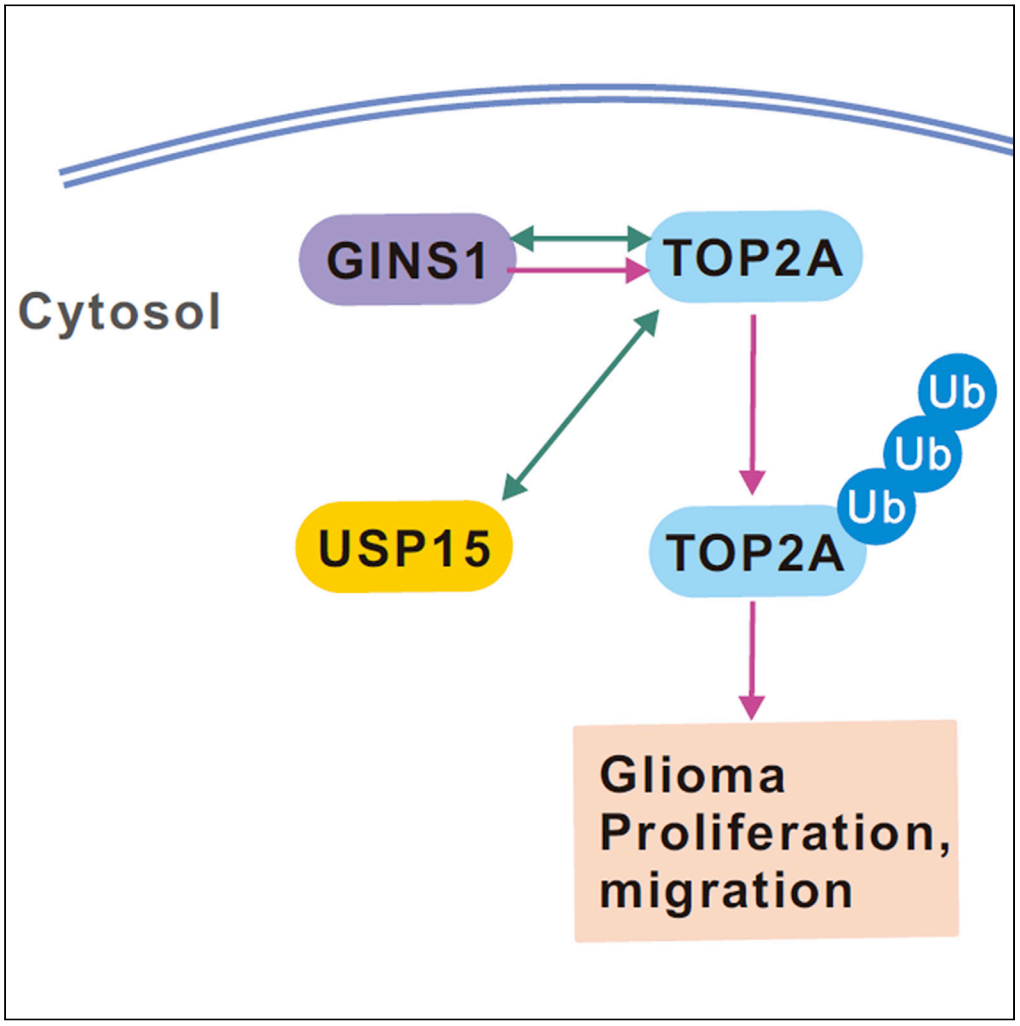

Hui Yang, Xiaocen Liu, Xiaolong Zhu, Mengying Zhang, Yingying Wang, Mingzhe Ma, Kun Lv

mmz666@163.com (M.M.)
lvkun315@126.com (K.L.)

Highlights

GINS1 expression was upregulated and associated with poor clinical outcome in glioma

GINS1 aggravated glioma malignant phenotypes *in vitro* and *in vivo*

GINS1 physically interacts with TOP2A

GINS1 regulates glioma progression through USP15-mediated deubiquitination of TOP2A

Yang et al., iScience *25*, 104952
September 16, 2022
https://doi.org/10.1016/j.isci.2022.104952

iScience

CellPress
OPEN ACCESS

Article

GINS1 promotes the proliferation and migration of glioma cells through USP15-mediated deubiquitination of TOP2A

Hui Yang,[1,2,3,4,8] Xiaocen Liu,[2,3,5,8] Xiaolong Zhu,[1,2,3,8] Mengying Zhang,[1,2,3] Yingying Wang,[5] Mingzhe Ma,[6,7,*] and Kun Lv[1,2,3,4,9,*]

SUMMARY

GINS1 is a GINS complex subunit that functions along with the MCM2-7 complex and Cdc45 in eukaryotic DNA replication. Despite the significance of the GINS complex in the switch between quiescence and proliferation of glioma cells inside and outside the perinecrotic niche, the biological functions and the underlying mechanism of GINS1 remain unclear. Unlike in normal cells and tissues, GINS1 expression level was significantly upregulated in glioma cells and tissues. High expression of GINS1 predicted an advanced clinical grade and a poor survival. Functional assays revealed that GINS1 aggravated glioma malignant phenotypes *in vitro* and *in vivo*. Mechanistically, this study identified that GINS1 physically interacts with TOP2A. GINS1 promotes glioma cell proliferation and migration through USP15-mediated deubiquitination of TOP2A protein. Our results delineate the clinical significance of GINS1 in glioma and the regulatory mechanisms involved in glioma cell proliferation and migration. This work provides potential therapeutic targets for glioma treatment.

INTRODUCTION

Glioma is the most common malignancy in the CNS, accounting for approximately 30% and 80% of all major nervous tumor cases and brain tumor cases, respectively (Siegel et al., 2021; Miller et al., 2021). Glioma is a lethal and aggressive cancer with high mortality and morbidity. According to the World Health Organization (WHO), gliomas are divided into four grades: pilocytic astrocytoma (WHO grade I), diffuse astrocytoma (WHO grade II), anaplastic astrocytoma (WHO grade III), and glioblastoma multiform (WHO grade IV) (Kristensen et al., 2019; Louis et al., 2016). Despite improvements and advances made in recent years in glioma treatment options, including surgical resection, radiation therapy, and chemotherapy, the prognosis of patients with glioma is still dismal (Silantyev et al., 2019). It has been estimated that the 5-year survival rate of patients with glioma is extremely low, which is even less than 10% for those with advanced WHO grades (Wen et al., 2020). Therefore, it is essential to uncover the detailed molecular mechanisms in glioma tumorigenesis and metastasis.

GINS family has four members, GINS5, GINS1, GINS2, and GINS3 (Go, Ichi, Nii, and San in Japanese for five, one, two, and three, respectively, in English). GINS1, also known as Partner of SLD Five 1 (PSF1), forms a heterotetramer complex with SLD5, PSF2, and PSF3. Through recruiting Cdc45 and DNA polymerase, this complex is essential for the initiation and elongation of DNA replication (Chang et al., 2007; Gambus et al., 2006; Kanemaki et al., 2003). GINS1 was initially found to be predominantly expressed in highly proliferating cells instead of mature cells. Later on, it was found that GINS was involved in the tumorigenesis of various cancers, including breast cancer, colorectal cancer, and hepatocellular carcinoma (Toda et al., 2020; Bu et al., 2020; Li et al., 2021). Although growing evidence has shown that the GINS complex serves as a switch between quiescence and proliferation of glioma cells inside and outside the perinecrotic niche (Kimura et al., 2019), the specific function of GINS1 and the underlying mechanism in glioma remain largely unknown.

Topoisomerases play a vital role in DNA world, being essentially involved in administering DNA topology (Wang, 2002). Topoisomerases show elevated levels of expression in tumor cells. There are total of six topoisomerases in humans, which include two enzymes in each subfamily: IA (TOP3A and TOP3B), IB (TOP1 and mitochondrial TOP1), and IIA (TOP2A and TOP2B) (Cuya et al., 2017; Hou et al., 2020). Topoisomerase

[1]Department of Central Laboratory, The First Affiliated Hospital of Wannan Medical College (Yijishan Hospital of Wannan Medical College), Wuhu 241001, China

[2]Key Laboratory of Non-coding RNA Transformation Research of Anhui Higher Education Institutes, Wannan Medical College, Wuhu 241001, China

[3]Non-coding RNA Research Center of Wannan Medical College, Wuhu 241001, China

[4]Anhui Province Clinical Research Center for Critical Respiratory Medicine, Wuhu 241001, China

[5]Department of Nuclear Medicine, the First Affiliated Hospital of Wannan Medical College (Yijishan Hospital of Wannan Medical College), Wuhu 241001, China

[6]Department of Gastric Surgery, Fudan University Shanghai Cancer Center, Shanghai 200032, China

[7]Department of Oncology, Shanghai Medical College, Fudan University, Shanghai 200032, China

[8]These authors contributed equally

[9]Lead contact

*Correspondence: mmz666@163.com (M.M.), lvkun315@126.com (K.L.)

https://doi.org/10.1016/j.isci.2022.104952

II alpha (TOP2A) is an enzyme involved in DNA maintenance and repair as well as cell proliferation (Albadine et al., 2009). By creating a DNA-linked protein gate through which another intact DNA duplex passes, TOP2A mainly supports DNA decoiling, chromosome segregation during cell cycle anaphase, and DNA replication that are necessary processes for cell proliferation (Schindlbeck et al., 2010), so TOP2A is also a cell proliferation marker in normal and neoplastic tissues (Shvero et al., 2008). TOP2A plays a critical role in glioma cell proliferation and migration (Song et al., 2018; Deguchi et al., 2017). In malignant cells, TOP2A protein overexpression might reflect the proliferative advantage of these cells and qualitative alterations caused by malignant transformation and dedifferentiation (Nakopoulou et al., 2001). The immunohistochemical (IHC) method for *in situ* determination of TOP2A has been extensively validated to reflect the exact enzyme activity closely in formalin-fixed paraffin-embedded human tissues, leading to the prognostic and predictive importance of this test in other neoplasms (Shamaa et al., 2008). Posttranslational modifications of TOP2A, including ubiquitylation, SUMOylation, and phosphorylation, have been implicated in the regulation of TOP2A localization, turnover, and activities (Nitiss, 2009; Chen et al., 2013; Vos et al., 2011). TOP2A ubiquitination by BMI1/RING1A or APC/C-Cdh1 promotes its degradation, while its ubiquitination by BRCA1 stimulates its decatenation activity and its proteasomal degradation (Alchanati et al., 2009; Eguren et al., 2014; Lou et al., 2005; Shinagawa et al., 2008). The reversal posttranslational modification of ubiquitylation, deubiquitylation, is also important in the regulation of TOP2A function (Chen et al., 2015). Despite the importance of ubiquitylation on TOP2A function and its steady-state levels, the mechanisms that mediate its deubiquitination in glioma cell proliferation and migration have not yet been identified.

Ubiquitination is a posttranslational protein modification process that attaches single or multiple ubiquitin molecules to a target protein and affects its stability and function. Ubiquitin conjugation is mediated by the sequential action of three enzymes, ubiquitin-activating enzyme (E1), ubiquitin-conjugating enzymes (E2s), and ubiquitin ligases (E3s) (Hershko and Ciechanover, 1998). Lysine (K) 48-linked polyubiquitin chains are the best-studied ubiquitin chains that target proteins for proteasomal degradation, whereas some other ubiquitin chains, such as the K63-linked polyubiquitin chains, can mediate nondegradative functions (Chen and Sun, 2009). The specificity of protein ubiquitination is regulated by E3 ubiquitin ligases, which exist in large numbers in mammalian cells and mediate substrate recognitions (Li et al., 2008). Ubiquitination is a reversible reaction since the ubiquitin chains can be cleaved by a large family of ubiquitin-specific proteases, termed deubiquitinases (Reyes-Turcu et al., 2009; Zou et al., 2014). Deubiquitinases can have specificity for both protein substrates and ubiquitin chains, thereby bringing in a different level of diversity in the regulation of ubiquitination. Deregulation of the deubiquitination process is frequently associated with tumorigenesis (Sun et al., 2020; Mevissen and Komander, 2017). Among deubiquitinases, ubiquitin-specific protease 15 (USP15) is a member of the largest subfamily of cysteine protease deubiquitinases (Mevissen and Komander, 2017). USP15 was previously reported to regulate TGF-β signaling and cancer cell survival. USP15 is aberrantly regulated or mutated in many human cancers, including glioma (Vos et al., 2009; Inui et al., 2011; Eichhorn et al., 2012). However, the detailed function of USP15, particularly in the regulation of glioma cell proliferation and migration, has remained unclear.

In the current study, we revealed that GINS1 was significantly upregulated in glioma cells and tissues. High expression of GINS1 predicted an advanced clinical grade and a poor survival. GINS1 exacerbated glioma malignant phenotypes *in vitro* and *in vivo*. Mechanistically, this study identified that GINS1 physically interacts with TOP2A and that GINS1 promotes glioma cell proliferation and migration through USP15-mediated deubiquitination of the TOP2A protein. Thus, our results, for the first time, identified a GINS1-USP15-TOP2A axis that regulates glioma cell proliferation and migration and will provide a potential therapeutic strategy for glioma.

RESULTS

GINS1 expression was significantly upregulated in glioma and associated with poor clinical glioma outcomes

Microarray expression profiling was performed to identify differentially expressed genes (DEGs) in 5 pairs of human glioma tissue specimens and corresponding adjacent nontumor tissue specimens. Several notably upregulated DEGs and downregulated DEGs existed between human glioma tissue specimens and corresponding adjacent nontumor tissue specimens (Figures 1A–1C). Eight candidate genes (SGK223, BORCS8, GINS1, UBTD2, THOC3, RFC4, HOXD4, and ANXA2P2) were further identified based on the Cancer Genome Atlas (TCGA) database and gene chip. High-content screening (HCS) analysis was introduced to verify these eight candidate genes in U251 cells. Among them, only GINS1 silencing outstandingly inhibited glioma cell proliferation (Figures 1D–1F), suggesting that GINS1 might be involved in glioma progression.

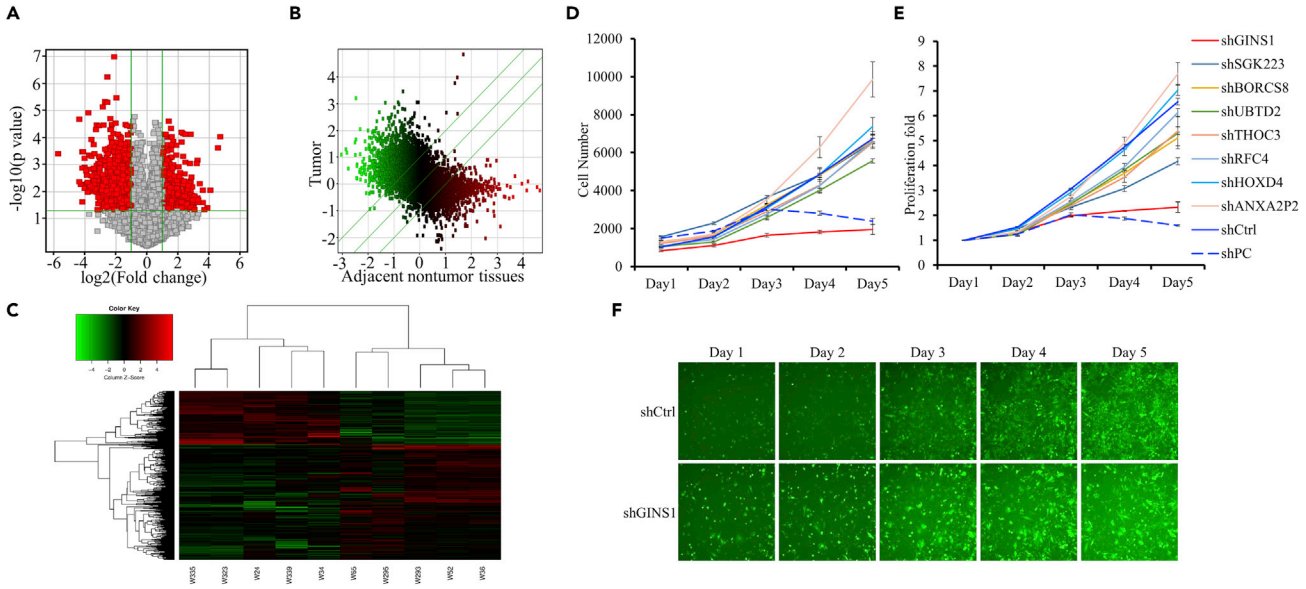

Figure 1. Gene expression profile analysis of GINS1 in gliomas

(A) Volcano map of differentially expressed genes in 10 human glioma tissues and corresponding adjacent noncancerous tissues. Red dots are the significant differentially expressed genes, and gray dots are the nonsignificant differentially expressed genes.

(B) Scatterplot of differentially expressed genes in 10 human glioma tissues and corresponding adjacent noncancerous tissues. The parallel green solid line is the difference reference line, and the points within the reference line represent the probe group with no significant change. Red points outside the reference line represent the probe group with relatively upregulated expression in the glioma tissue group, and green points represent the probe group with relatively upregulated expression in the adjacent noncancerous tissue group.

(C) Clustering analysis of differentially expressed genes in 10 human glioma tissues and corresponding adjacent noncancerous tissues. Red indicates that the gene expression level is relatively upregulated, green indicates that the gene expression level is relatively downregulated, black indicates that there is no significant change in gene expression, and gray indicates that the signal intensity of the gene is not detected.

(D–F) The effect of GINS1 inhibition on cell proliferation was detected by high-content screening (HCS). All data are presented as the mean ± SD.

To explore GINS1 expression in glioma, we first used TCGA database to show that GINS1 expression was increased in glioma (n = 156), compared with other normal brain tissues (n = 5) (Figure 2A). We then compared GINS1 expression level between four human glioma cell lines and one normal human glial cell line, HEB by RT-PCR and Western blot analyses. We found that GINS1 mRNA and protein levels were upregulated in four human glioma cell lines, T98G, U251, U373, and A172, compared with HEB (Figures 2B and 2C). Next, we sought to examine the expression level of GINS1 first in four pairs and then in 80 pairs of our human glioma tissue and adjacent noncancerous tissues that we collected. GINS1 expression levels detected by Western blotting was increased more significantly in four human glioma tissue samples, compared with levels in four adjacent noncancerous tissues (Figure 2D). Furthermore, RT-PCR and Western blot analyses were utilized to detect GINS1 expression in 80 paired glioma and adjacent noncancerous tissues. The expression patterns of GINS1 between these 80 paired samples were found to be similar to that of four paired samples. The expression level of GINS1 is positively correlated with the tumor clinical stage (Figures 2E and 2F). In order to examine the spatial expression level of GINS1, we next used tissue microarrays and IHC to analyze the protein level of GINS1 between glioma tissues and normal brain samples. Similar to the mRNA results, the IHC staining intensity of GINS1 protein was positively correlated with the tumor clinical stage (Figure 2G). GINS1 protein expression in glioma tissues was also higher than that in matched adjacent noncancerous tissues (Figure 2H). Kaplan–Meier survival analysis from TCGA and CGGA databases showed that patients with glioma with high GINS1 expression had poorer overall survival (OS), progression-free survival (PFS), and disease-free survival rates (DFS) than patients with glioma with low GINS1 expression (Figures 2I–2K and S1A–S1C). Similar results were obtained in the specimens of the validation cohort of patients with glioma from our laboratory (Figures S1D and S1E). The clinicopathological analysis indicated that age and tumor stage were also associated with the GINS1 variable (chi-square test, p = 0.001). In contrast, cell differentiation grade of glioma and gender exhibited no significant correlation with GINS1 expression level (Table 1). These data indicated that GINS1 was upregulated in glioma and correlated with the clinicopathological features and poor prognosis of patients with glioma.

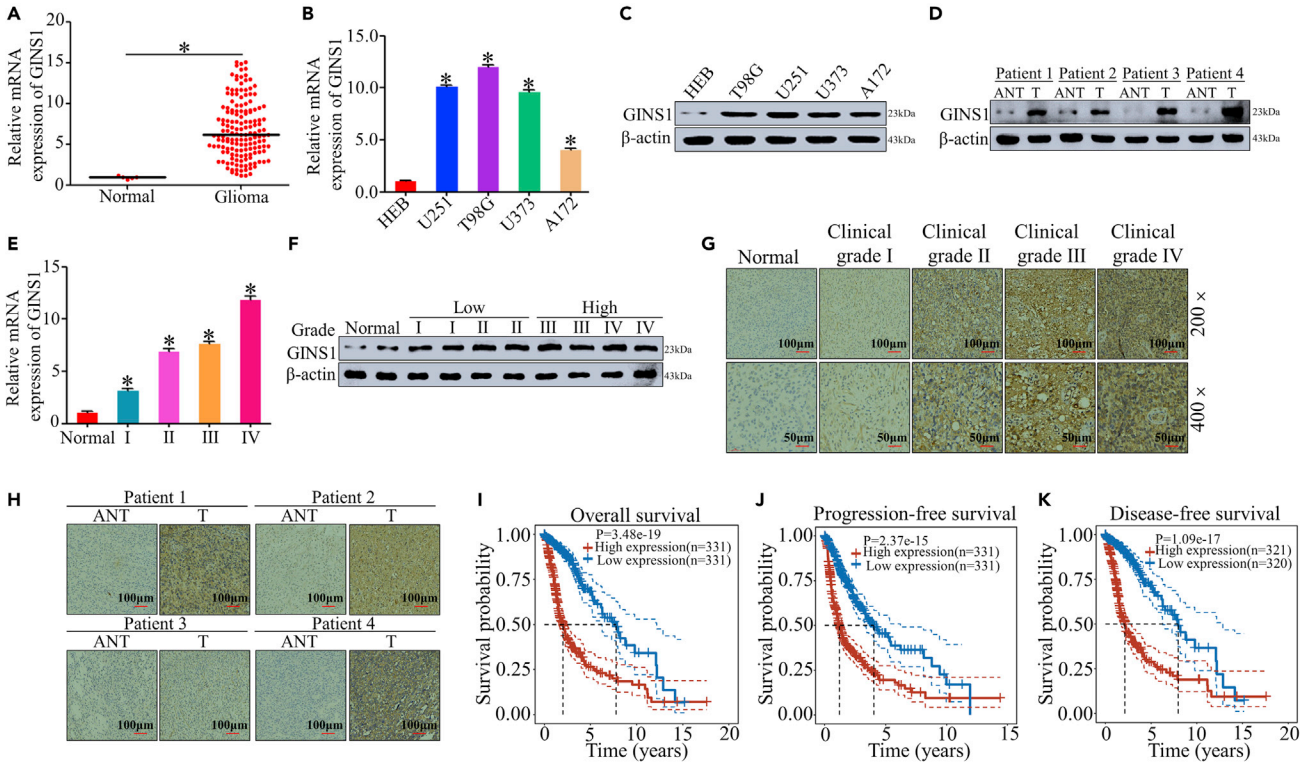

Figure 2. GINS1 expression was significantly upregulated in glioma and associated with poor clinical glioma outcomes

(A) Relative GINS1 mRNA expression in normal brain tissues (n = 5) and glioma tissues (n = 156) acquired from TCGA database. Bar graph data are presented as the mean ± SD; *, $p < 0.05$.

(B) Relative GINS1 mRNA expression in normal brain cell (HEB) and glioma cell lines (T98G, U251, U373, and A172) measured by real-time PCR. Bar graph data are presented as the mean ± SD; *, $p < 0.05$.

(C) Western blot analysis of GINS1 expression in normal brain cells (HEB) and glioma cell lines (T98G, U251, U373, and A172). β-actin was used as a loading control.

(D) Western blot analysis of GINS1 expression in matched primary glioma tissues (T) and adjacent noncancerous tissues (ANT). The patients were clinically grade characterized (patient #1: Grade III; patient #2: Grade II; patient #3: Grade I; patient #4: Grade IV). β-actin was used as a loading control.

(E) Relative GINS1 mRNA expression in glioma specimens of low clinical grades and high clinical grades determined by real-time PCR. Bar graph data are presented as the mean ± SD; *, $p < 0.05$.

(F) Western blot analysis of GINS1 expression in glioma specimens of low clinical grades and high clinical grades. β-actin was used as loading control.

(G) IHC staining analysis of GINS1 protein expression in normal brain tissues and glioma tissues of different clinical stages. Scale bars, 100 μm (200× magnification) for upper panels and 50 μm (400× magnification) for lower panels.

(H) IHC staining analysis of GINS1 protein expression in matched primary glioma tissues (T) and adjacent noncancerous tissues (ANT). The patients were clinically grade characterized (patient #1: Grade III; patient #2: Grade II; patient #3: Grade I; patient #4: Grade IV). Scale bars, 100μm(200×magnification) for all panels.

(I) Kaplan–Meier survival curves show the overall survival of high GINS1-expressing (n = 331) and low GINS1-expressing (n = 331) patients with glioma from the TCGA database.

(J) Kaplan–Meier survival curves show progression-free survival of high GINS1-expressing (n = 331) and low GINS1-expressing (n = 331) patients with glioma from the TCGA database.

(K) Kaplan–Meier survival curves show disease-free survival of high GINS1-expressing (n = 321) and low GINS1-expressing (n = 320) patients with glioma from the TCGA database.

GINS1 silencing suppresses glioma cell proliferation, migration, and invasion, but promotes glioma cell apoptosis *in vitro* and *in vivo*

Two lentiviruses expressing shRNAs were constructed to silence GINS1 expression in U251 and T98G cells to investigate the functional role of GINS1 in glioma cells (Figures 3A–3D). The MTT assay demonstrated that GINS1 silencing markedly inhibited cell proliferation (Figures 3E, 3F, S2A, and S2B). Colony formation assays indicated that silencing GINS1 expression resulted in much smaller and fewer colonies (Figures 3G and 3H). In addition, Transwell assay and wound healing assay showed that GINS1 silencing dramatically decreased glioma cell migration and invasion, respectively (Figures 3I and 3J). Given that matrix metallo-proteinase 9 (MMP-9) protein and EMT-related proteins participated in tumor cell proliferation, migration,

Table 1. Correlation between GINS1 expression and clinicopathological characteristics of the patients with glioma

	GINS1 expression			
Characteristics	Cases	High (%)	Low (%)	P
Age (years)				0.001
≤50	121	90(74.38)	31 (25.62)	
>50	52	44 (84.62)	8 (15.38)	
Gender				0.199
Male	109	84 (77.06)	25(22.94)	
Female	64	33 (51.56)	31 (48.44)	
Differentiation				
Well-moderate	81	55 (67.90)	26 (32.1)	0.211
Poor	92	62 (67.39)	30 (32.61)	
Tumor stages				0.001
I + II	102	7 (6.73)	97 (93.27)	
III + IV	71	72 (96.00)	3 (4.00)	

and invasion, the protein levels of MMP9, N-cadherin, Vimentin, and E-cadherin in GINS1-silenced U251 and T98G cells were measured. GINS1 silencing decreased the expression levels of N-cadherin, Vimentin, and MMP9 but enhanced the E-cadherin expression level in U251 and T98G cells (Figures 3K and 3L). These observations demonstrate that GINS1 silencing suppresses the proliferation, migration, and invasion of glioma cells. Then, the impact of GINS1 on cell apoptosis was assessed through flow cytometry. After GINS1 silencing, the percentage of apoptotic cells was significantly increased (Figures 3M and 3N). Additionally, GINS1 silencing decreased the expression levels of the antiapoptotic proteins Bcl-2 and Bcl-xl but enhanced the proapoptotic protein BAX in U251 and T98G cells (Figures 3O and 3P). Furthermore, we found that GINS1 silencing has no influence on the proliferation, migration, invasion, and apoptosis of the normal glial cell HEB (Figures S3A–S3I). The xenograft tumor model was generated to determine whether GINS1 contributes to tumor progression *in vivo*. GINS1 shRNA (shGINS1#1)-transfected tumor cells and control shRNA (shCtrl)-transfected cells were established and then injected subcutaneously into the right dorsal flanks of the nude mice. After 5 weeks of injection, the tumor volume and tumor weight of the shGINS1#1 group were significantly reduced compared to those of the shCtrl group (Figures 4A–4C). We found that downregulated Ki67 expression levels were detected in the GINS1-silenced group by immunohistochemistry (Figure 4D). These findings indicated that GINS1 silencing suppressed glioma cell proliferation, migration, and invasion, but promoted glioma cell apoptosis *in vitro* and *in vivo*.

GINS1 overexpression promotes the proliferation, migration, and invasion of glioma cells, but suppresses apoptosis of glioma cells *in vitro* and *in vivo*

To further explore the biological role of overexpressed GINS1 in glioma, the glioma cell line A172 with GINS1 overexpression was established (Figures 4E and 4F). MTT assay and colony formation assay showed that GINS1 overexpression significantly promoted glioma cell proliferation (Figures 4G, 4H, and S2C), while Transwell assay and wound healing assay proved that GINS1 overexpression dramatically increased the invading and migrating abilities of glioma cells, respectively (Figures 4I and 4J). Next, the effects of GINS1 overexpression on cell apoptosis were further investigated. The percentage of apoptotic cells significantly decreased in GINS1-overexpressing A172 cells (Figure 4K). Figures 4L and 4M show that GINS1-overexpressing (GINS1 cDNA-transfected) A172 cells displayed higher MMP9, N-cadherin, Vimentin, Bcl-2, and Bcl-xl expression levels and lower levels of E-cadherin and BAX than control plasmid (pcDNA3.1)-transfected A172 cells (Figures 4L and 4M). Glioma cells with an endogenous or overexpressed GINS1 expression level were subcutaneously injected into the left flank of nude mice under the same conditions used for a xenograft tumor model of GINS1-silenced glioma cells to investigate the biological role of overexpressed GINS1 in glioma *in vivo*. The tumors formed by GINS1-overexpressing A172 cells had larger tumor volumes and heavier tumor weights than those induced by control plasmid (pcDNA3.1)-transfected A172 cells (Figures 4N–4P). In addition, the Ki67 expression level was upregulated in the tumors formed by GINS1-overexpressing glioma cells compared with those induced by control plasmid (pcDNA3.1)-transfected A172 cells (Figure 4Q). These above results revealed that overexpressed GINS1

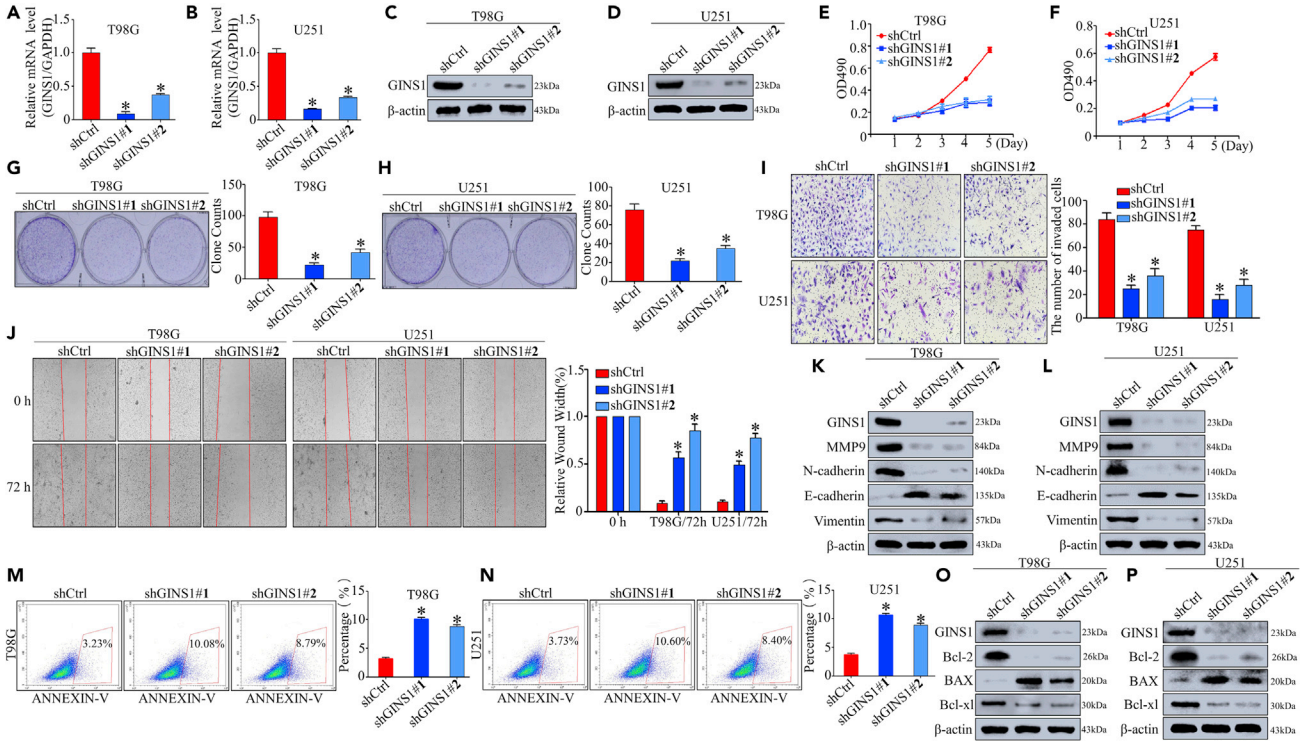

Figure 3. GINS1 silencing suppresses glioma cell proliferation, migration, and invasion and promotes glioma cell apoptosis *in vitro* and *in vivo*

(A and B) Relative GINS1 mRNA expression in T98G and U251 cells expressing GINS1 shRNA#1 and GINS1 shRNA#2 analyzed by real-time PCR. Experiments were conducted independently thrice. Bar graph data are presented as the mean ± SD; *, $p < 0.05$.

(C and D) Western blot analysis of GINS1 expression in GINS1-silenced T98G and GINS1-silenced U251 cells. β-actin was used as loading control.

(E–H) Cell proliferation was examined by MTT (E, F) and colony formation assays (G, H) in GINS1-silenced T98G and GINS1-silenced U251 cells. Representative pictures are shown on the left, and the number of colonies counted was shown on the right. Experiments were performed independently thrice. Bar graph data are presented as the mean ± SD; *, $p < 0.05$. Scale bars, 1 cm.

(I and J) The invasion and migration capacities of glioma cells were evaluated with transwell assays (I) and wound healing assays (J) in GINS1-silenced T98G and GINS1-silenced U251 cells. Representative pictures are shown on the left, and the statistical data are counted on the right. Experiments were performed independently thrice. Bar graph data are presented as the mean ± SD; *, $p < 0.05$. Scale bars, 200 μm.

(K and L) Western blot analysis of the expression level of MMP-9 protein and EMT-related proteins in GINS1-silenced T98G and GINS1-silenced U251 cells. β-actin was used as loading control.

(M and N) FACS assay was used to detect the apoptotic cells in GINS1-silenced T98G and GINS1-silenced U251 cells. Representative profiles are shown on the left, and the percentage of apoptotic cells was statistically analyzed on the right. Experiments were conducted independently thrice. Bar graph data are presented as the mean ± SD; *, $p < 0.05$.

(O and P) Western blot analysis of the expression level of crucial cell apoptosis regulatory proteins in GINS1-silenced T98G and GINS1-silenced U251 cells. β-actin was used as loading control.

significantly promoted the proliferation, migration, and invasion of glioma cells, but suppressed apoptosis of glioma cells *in vitro* and *in vivo*.

GINS1 physically interacts with TOP2A, while GINS1 induces glioma cell proliferation and migration in a TOP2A-dependent manner

We have proven that GINS1 silencing can suppress glioma cell proliferation and migration abilities. However, the specific regulatory mechanism signifying these effects is still unclear. Therefore, we performed affinity purification, silver staining, and LC-MS/MS assays to identify GINS1-associated proteins. The results revealed that TOP2A was a potential GINS1-interacting protein (Figure 5A) and verified by immunoprecipitation (Figure 5B), co-immunoprecipitation analysis (Figure 5C), and GST pull-down experiments of immunoprecipitated samples (Figure 5D). Detailed results from the mass spectrometric analysis are provided in Table S4. These experiments suggested that GINS1 physically interacts with TOP2A. TOP2A is an enzyme that controls the DNA topology and plays a critical role in glioma cell proliferation and migration (Albadine et al., 2009; Song et al., 2018; Deguchi et al., 2017). Thus, we examined whether GINS1 exerts oncogenic effects on glioma cell proliferation and

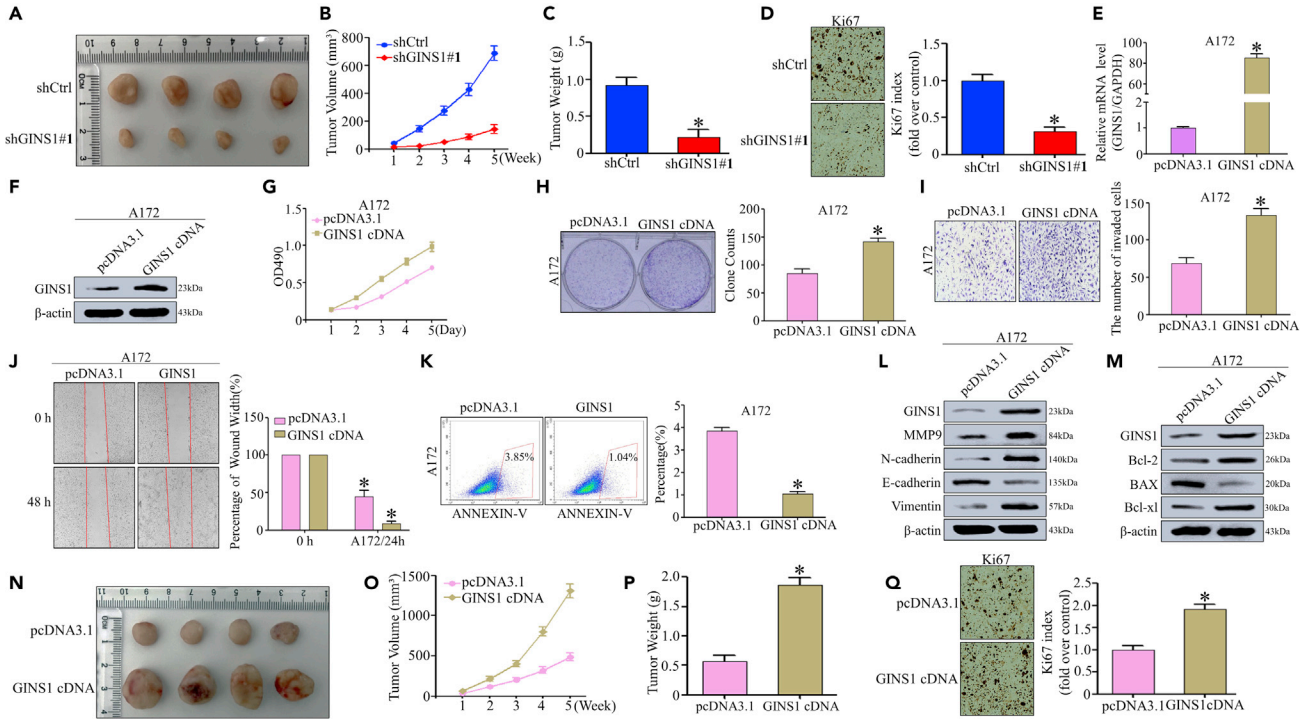

Figure 4. Overexpressed GINS1 promoted the proliferation, migration, and invasion of glioma cells *in vitro* and *in vivo*

(A) Representative images of the corresponding xenografts in the shCtrl and shGINS1 groups.

(B) The growth curve of the tumors in the shCtrl and shGINS1 groups. Bar graph data are presented as the mean ± SD; *, $p < 0.05$.

(C) The weight of tumors in the shCtrl and shGINS1 groups. Bar graph data are presented as the mean ± SD; *, $p < 0.05$.

(D) The Ki67 expression level was determined in xenograft model tumor tissues using immunohistochemical staining. All data are presented as the mean ± SD; *, $p < 0.05$. Scale bars, 100 μm (200×magnification) for panels.

(E) Relative GINS1 mRNA expression in GINS1-overexpressing A172 cells investigated by real-time PCR. Experiments were conducted in triplicate. Bar graph data are presented as the mean ± SD; *, $p < 0.05$.

(F) Western blot analysis of GINS1 expression in GINS1-overexpressing A172 cells. β-actin was used as loading control.

(G, H) Cell proliferation was examined by MTT (G) and colony formation assays (H) in GINS1-overexpressing A172 cells. Representative pictures are shown on the left, and the number of colonies counted was shown on the right. Experiments were performed independently thrice. Bar graph data are presented as the mean ± SD; *, $p < 0.05$. Scale bars, 1 cm.

(I, J) The invasion and migration capacities of glioma cells were evaluated with transwell assays (I) and wound healing assays (J) in GINS1-overexpressing A172 cells. Representative pictures are shown on the left, and the statistical data are counted on the right. Experiments were performed independently thrice. Bar graph data are presented as the mean ± SD; *, $p < 0.05$. Scale bars, 200 μm.

(K) FACS assay was used to detect the apoptotic cell in GINS1-overexpressing A172 cells. Representative profiles are shown on the left, and the percentage of apoptotic cells was statistically analyzed on the right. Experiments were conducted independently thrice. Bar graph data are presented as the mean ± SD; *, $p < 0.05$.

(L) Western blot analysis of the expression level of MMP-9 protein and EMT-related proteins in GINS1-overexpressing A172 cells. β-actin was used as loading control.

(M) Western blot analysis of the expression level of crucial cell apoptosis regulatory proteins in GINS1-overexpressing A172 cells. β-actin was used as loading control.

(N) Representative images of the corresponding xenografts in the pcDNA3.1 and GINS1 cDNA groups.

(O) The growth curve of the tumors in the pcDNA3.1 and GINS1 cDNA groups. Bar graph data are presented as the mean ± SD; *, $p < 0.05$.

(P) The weight of tumors in the pcDNA3.1 and GINS1 cDNA groups. Bar graph data are presented as the mean ± SD; *, $p < 0.05$.

(Q) The Ki67 expression level was determined in xenograft model tumor tissues using immunohistochemical staining. All data are presented as the mean ± SD; *, $p < 0.05$. Scale bars, 100 μm (200×magnification) for all panels.

migration in a TOP2A-dependent manner. To explore the role of GINS1 in regulating TOP2A expression, we examined TOP2A protein levels in cells by varying GINS1 expression levels. GINS1 depletion significantly decreased TOP2A protein level in U251 cells, whereas GINS1 overexpression considerably elevated TOP2A protein levels in A172 cells (Figure 5E). Notably, no statistically significant changes in TOP2A mRNA levels were observed between these groups (Figure 5F), which suggests that GINS1 modulates TOP2A expression posttranscriptionally. Similarly, exogenous GINS1 expression in HEK293T cells dramatically elevated

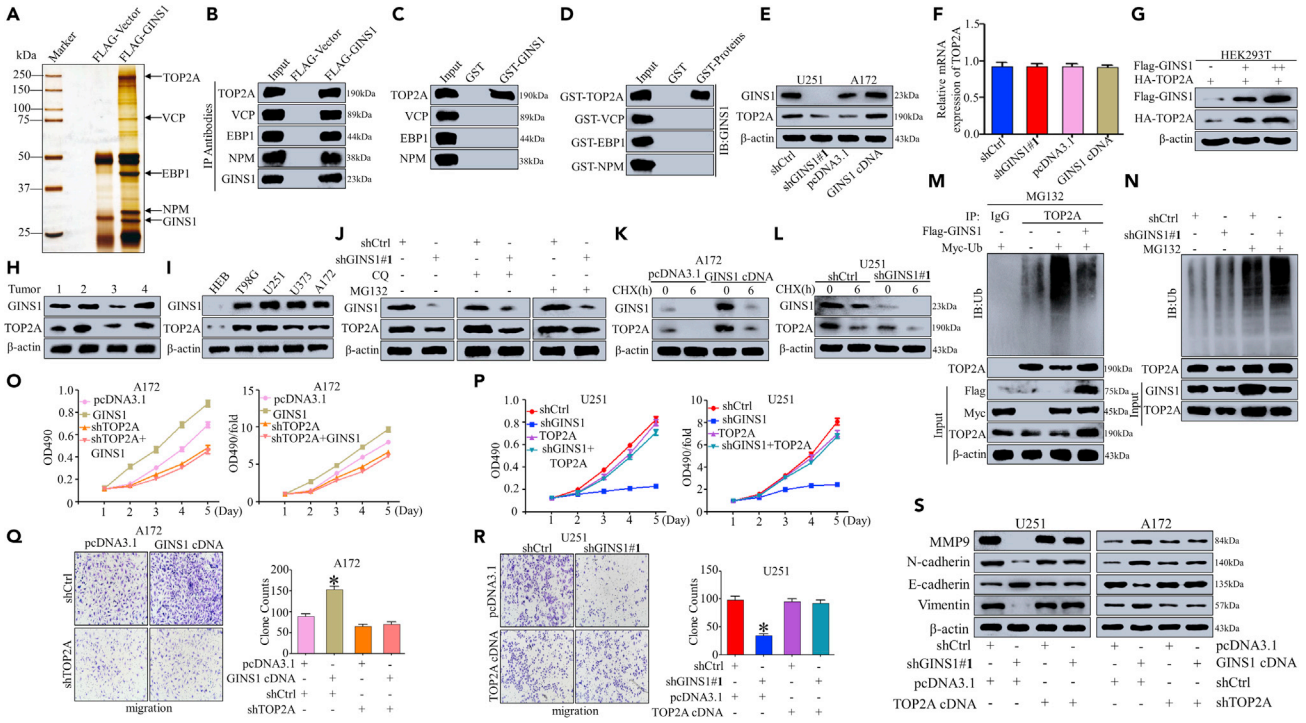

Figure 5. GINS1 physically interacts with TOP2A, while GINS1 induces glioma cell proliferation and migration in a TOP2A-dependent manner

(A) Immunoaffinity purification and mass spectrometry analysis of GINS1-containing protein n complexes. Cellular extracts from U251 cells stably expressing FLAG (Vector) or FLAG-GINS1 were immunopurified with anti-FLAG affinity columns and eluted with FLAG peptide. The eluates were resolved by SDS–PAGE and silver-stained. The protein bands were retrieved and analyzed by mass spectrometry. Detailed results from the mass spectrometric analysis are provided in Table S4.

(B) IP of whole-cell lysates from U251 cells followed by IB with antibodies against the indicated proteins.

(C) GST pull-down assays with GST-fused GINS1 and *in vitro* transcribed/translated TOP2A, VCP, EBP1, and NPM as indicated.

(D) GST pull-down assays with the indicated GST-fused proteins and *in vitro* transcribed/translated GINS1.

(E) WB analysis of TOP2A and USP15 expression in GINS1-silenced U251 cells and GINS1-overexpressing A172 cells.

(F) Relative TOP2A mRNA expression in GINS1-silenced U251 cells and GINS1-overexpressing A172 cells measured by real-time PCR. Bar graph data are presented as the mean ± SD.

(G) Western blot analysis of exogenous TOP2A in HEK293T cells co-expressing GINS1 and TOP2A.

(H) Western blot analysis of the protein levels of GINS1 and TOP2A in clinical glioma specimens.

(I) Western blot analysis of the protein levels of GINS1 and TOP2A in normal brain cells (HEB) and glioma cell lines (T98G, U251, U373, and A172).

(J) Western blot analysis of TOP2A levels in GINS1-silenced U251 cells treated with MG132 and CQ.

(K and L) CHX chase analysis of TOP2A protein half-life in GINS1-overexpressing A172 cells and GINS1-silenced U251 cells.

(M and N) Ubiquitination assays of endogenous TOP2A in lysates from A172 cells transfected with Flag-GINS1 (M) or U251 cells stably expressing GINS1 shRNA (N).

(O and P) Stable GINS1 overexpression (A172-GINS1) cells were transfected with TOP2A shRNA, and stable GINS1 knockdown (U251-shRNA) cells were transfected with TOP2A cDNA. The role of TOP2A in GINS1-induced proliferation was examined by MTT assays. Bar graph data are presented as the mean ± SD; *, $p < 0.05$.

(Q and R) Transwell assays detected the effect of TOP2A on GINS1-induced migration. Representative pictures are shown on the left, and the statistical data are counted on the right. Experiments were performed independently thrice. Bar graph data are presented as the mean ± SD; *, $p < 0.05$. Scale bars, 200 μm.

(S) Western blot analysis of the expression level of MMP-9 protein and EMT-related proteins in co-transfected U251 and A172 cells.

exogenous TOP2A protein levels in a dose-dependent manner (Figure 5G). In addition, GINS1 expression levels were positively correlated with TOP2A protein levels in four glioma clinical specimens and glioma cells of five cell lines (Figures 5H and 5I). Then, we speculated that GINS1 might regulate the degradation pathway of the TOP2A protein. The autophagolysosome and ubiquitin–proteasome pathways are the main protein degradation pathways, so glioma cells were treated with ubiquitin–proteasome and autophagolysosome pathway inhibitors MG132 and chloroquine diphosphate (CQ), respectively. The results showed that MG132 could, to a certain extent, reverse GINS1 regulation of TOP2A protein (Figure 5J). The TOP2A abundance in glioma cells treated with cycloheximide (CHX), a *de novo* protein synthesis inhibitor, was detected to examine whether GINS1 regulates TOP2A protein stability. GINS1 overexpression in A172 cells significantly increased the

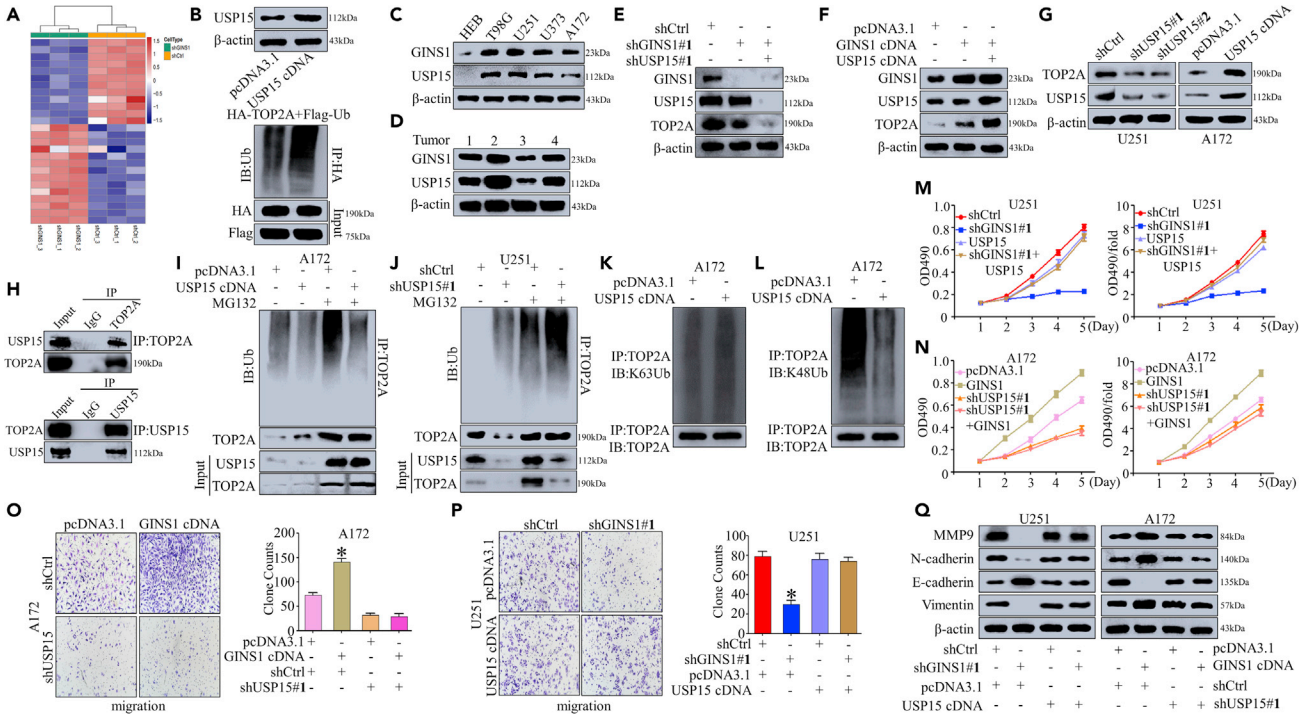

Figure 6. GINS1 promotes glioma cell proliferation and migration by USP15-mediated deubiquitination of TOP2A

(A) Microarray analysis of mRNAs was performed with RNA extracted from U251 shCtrl and U251 shGINS1 cells.

(B) Ubiquitination assays of endogenous TOP2A in HEK293T cells co-transfected with HA-TOP2A, Flag-Ub, and USP15.

(C) Western blot analysis of the protein levels of GINS1 and USP15 in normal brain cells (HEB) and glioma cell lines (T98G, U251, U373, and A172).

(D) Western blot analysis of the protein levels of GINS1 and USP15 in clinical glioma specimens and human glioma cell lines.

(E) Western blot analysis of the protein levels of GINS1, TOP2A, and USP15 in GINS1-silenced U251 cells transfected with USP15 shRNA. (F) Western blot analysis of the protein levels of GINS1, TOP2A, and USP15 in GINS1-overexpressing A172 cells transfected with USP15 cDNA.

(G) Western blot analysis of the protein levels of TOP2A and USP15 in U251 cells transfected with two independent USP15 shRNAs and A172 cells expressing USP15 cDNA.

(H) Reciprocal Co-IP and Western blot assays indicated an interaction between endogenous USP15 and TOP2A in A172 cells.

(I and J) Ubiquitination assays of endogenous TOP2A in lysates from A172 cells transfected with USP15 cDNA (I) or U251 cells transfected with USP15 shRNA (J).

(K and L) U251 cells were transfected with USP15 cDNA for 48 h, and cells were collected for lysate preparation and IP/IB assays as indicated.

(M and N) Stable GINS1 overexpression (A172-GINS1) cells were transfected with USP15 shRNA, and stable GINS1 knockdown (U251-shRNA) cells were transfected with USP15 cDNA. The role of USP15 in GINS1-induced proliferation was examined by MTT assays. Bar graph data are presented as the mean ± SD; *, $p < 0.05$.

(O and P) Transwell assays detected the effect of USP15 on GINS1-induced migration. Representative pictures are shown on the left, and the statistical data are counted on the right. Experiments were performed in triplicate. Bar graph data are presented as the mean ± SD; *, $p < 0.05$. Scale bars, 200 μm.

(Q) Western blot analysis of the expression level of MMP-9 protein and EMT-related proteins in co-transfected U251 and A172 cells.

stability of TOP2A (Figure 5K). Accordingly, the silencing of GINS1 in U251 cells greatly destabilized the TOP2A protein (Figure 5L). The role of GINS1 in TOP2A ubiquitination was further identified. In the presence or absence of MG132, enforced GINS1 expression inhibited TOP2A ubiquitination, whereas GINS1 silencing promoted TOP2A ubiquitination (Figures 5M and 5N). The above data all showed that GINS1 stabilized the TOP2A protein by inhibiting its ubiquitination.

To further explore whether GINS1 induces the proliferation and invasion of glioma cells in a TOP2A-dependent manner, either a specific TOP2A plasmid or shRNA was utilized to conduct studies on U251 and A172 cells. The effects of TOP2A shRNA and plasmid on proliferation and migration were also examined. TOP2A shRNA impaired cell proliferation in GINS1-overexpressing A172 cells. In contrast, the TOP2A plasmid rescued the diminished cell proliferation in GINS1-silenced U251 cells (Figures 5O and 5P). A Transwell assay was then conducted to explore the effect of TOP2A plasmid or shRNA on glioma cell migration. The results showed that TOP2A shRNA attenuated cell migration in GINS1-overexpressing A172 cells, whereas TOP2A plasmid recovered the diminished cell migration in GINS1-silenced U251 cells

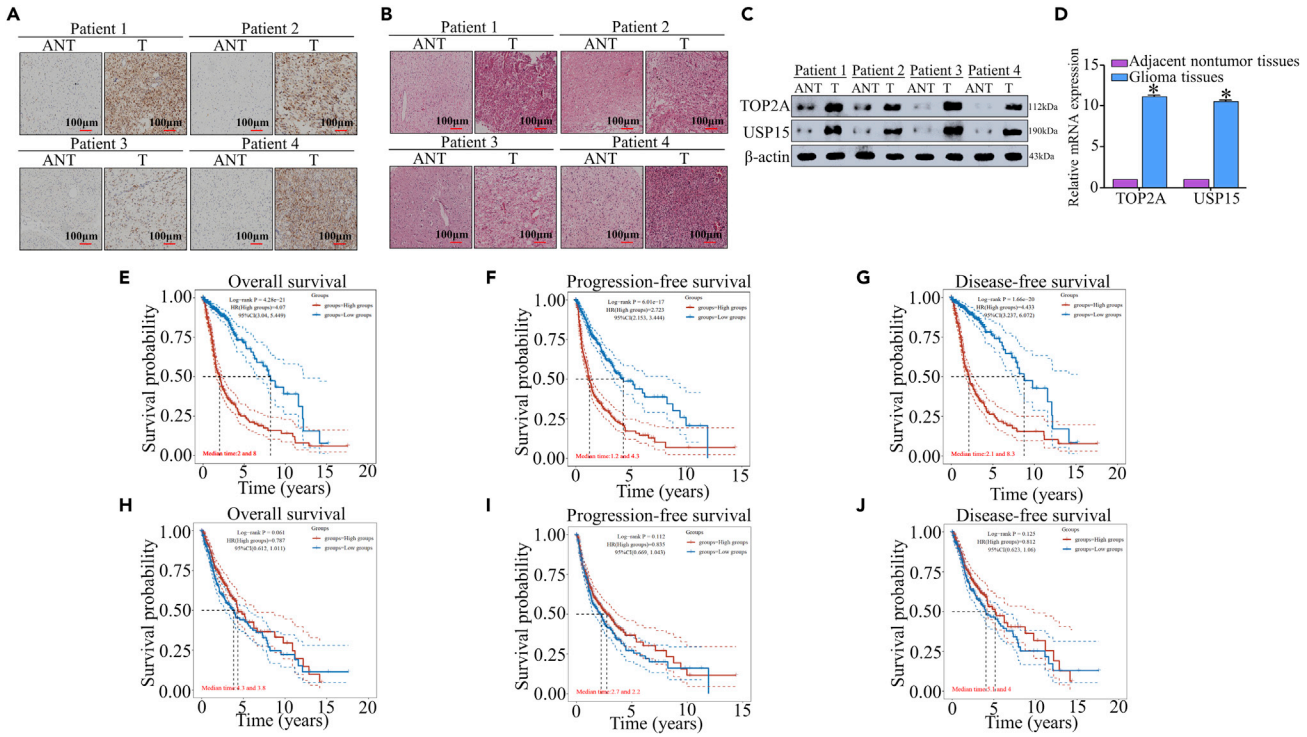

Figure 7. Both TOP2A and USP15 are upregulated in glioma and correlated with poor prognosis

(A and B) IHC staining analysis of TOP2A (A) and USP15 (B) protein expression in matched primary glioma tissues (T) and adjacent noncancerous tissues (ANT). The patients were clinically grade characterized (patient #1: Grade III; patient #2: Grade II; patient #3: Grade I; patient #4: Grade IV). Scale bars, 100 μm (200×magnification) for all panels.

(C) Western blot analysis of TOP2A and USP15 expression in matched primary glioma tissues (T) and adjacent noncancerous tissues (ANT). The patients were clinically grade characterized (patient #1: Grade III; patient #2: Grade II; patient #3: Grade I; patient #4: Grade IV). β-actin was used as a loading control.

(D) RT–PCR analysis of TOP2A and USP15 mRNA expression in matched primary glioma tissues (T) and adjacent noncancerous tissues (ANT). Experiments were performed independently thrice. Bar graph data are presented as the mean ± SD; *, $p < 0.05$.

(E) Kaplan–Meier survival curves show the overall survival of patients with glioma with high TOP2A expression (n = 331) and low TOP2A expression (n = 331) from the TCGA database.

(F) Kaplan–Meier survival curves show progression-free survival of high TOP2A-expressing (n = 331) and low TOP2A-expressing (n = 331) patients with glioma from the TCGA database.

(G) Kaplan–Meier survival curves show disease-free survival of patients with glioma with high TOP2A expression (n = 321) and low TOP2A expression (n = 320) from the TCGA database.

(H) Kaplan–Meier survival curves show the overall survival of patients with glioma with high USP15 expression (n = 331) and low USP15 expression (n = 331) from the TCGA database.

(I) Kaplan–Meier survival curves show progression-free survival of high USP15-expressing (n = 331) and low USP15-expressing (n = 331) patients with glioma from the TCGA database.

(J) Kaplan–Meier survival curves show disease-free survival of high USP15-expressing (n = 321) and low USP15-expressing (n = 320) patients with glioma from the TCGA database.

(Figures 5Q and 5R). Furthermore, we used Western blotting to analyze the protein levels of MMP9, N-cadherin, Vimentin, and E-cadherin in GINS1-silenced U251 and GINS1-overexpressing A172 cells. Figure 5S shows that TOP2A shRNA impaired the protein levels of MMP9, N-cadherin, and Vimentin, but recovered E-cadherin expression in GINS1-overexpressing A172 cells, while TOP2A plasmid restored the protein levels of MMP9, N-cadherin, and Vimentin, but attenuated E-cadherin expression in GINS1-silenced U251 cells (Figure 5S). These observations demonstrate that GINS1 induced the proliferation and migration of glioma cells in a TOP2A-dependent manner.

GINS1 promotes glioma cell proliferation and migration by USP15-mediated deubiquitination of TOP2A

Posttranslational modifications, including deubiquitination, are important regulators of TOP2A function (Chen et al., 2015). GINS1 mainly serves as a relevant factor of DNA replication and is unlikely to act

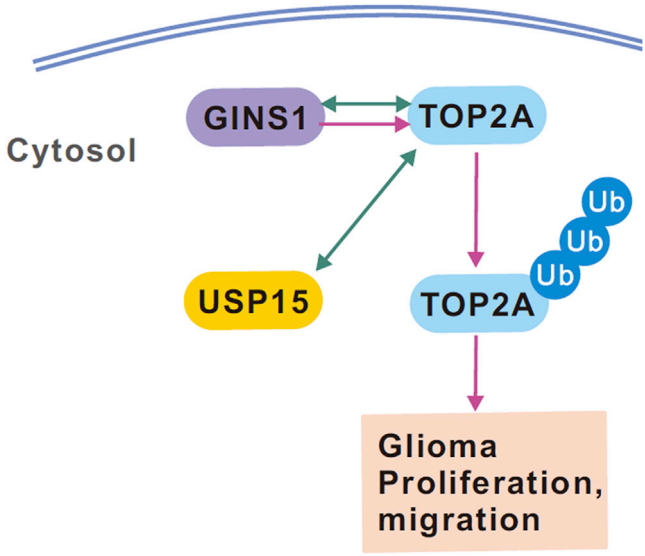

Figure 8. Schematic diagram of the molecular mechanism by which GINS1 promotes the proliferation and migration of glioma cells

Schematic diagram of the molecular mechanism by which GINS1 promotes the proliferation and migration of glioma cells. GINS1 physically interacts with TOP2A, and TOP2A physically interacts with USP15. GINS1 promotes glioma cell proliferation and migration through USP15-mediated ubiquitination of the TOP2A protein.

directly as a deubiquitinase to mediate TOP2A ubiquitination. Therefore, it was speculated that some deubiquitinases might be responsible for the TOP2A ubiquitination induced by GINS1. mRNA microarray analysis was conducted using total RNA isolated from U251 shCtrl- and U251 shGINS1-transfected cells (n = 3), and USP15 was screened as the top of the differentially expressed deubiquitinase genes (Figure 6A). Then, the influence of USP15 on TOP2A ubiquitination was identified. The results revealed that USP15 significantly diminished TOP2A ubiquitination, suggesting that USP15 might be a potential TOP2A deubiquitinase (Figure 6B). Simultaneously, USP15 protein expression was actively correlated with GINS1 protein levels in glioma cell lines and tissues (Figures 6C and 6D). Moreover, USP15 knockdown enhanced the TOP2A inhibition induced by GINS1 silencing and USP15 overexpression promoted the upregulation of TOP2A expression induced by GINS1 overexpression (Figures 6E and 6F). Next, the effect of USP15 on TOP2A protein expression was examined. As shown in Figure 6G, TOP2A depletion in U251 cells significantly reduced USP15 protein expression. In contrast, enhanced TOP2A expression in A172 cells dramatically upregulated USP15 protein levels (Figure 6G). Furthermore, the impact of USP15 on TOP2A ubiquitination was assessed. USP15 overexpression significantly promoted the endogenous ubiquitination of TOP2A in A172 cells (Figure 6G). We further investigated the interaction between USP15 and TOP2A. Reciprocal co-immunoprecipitation analysis demonstrated that endogenous USP15 and TOP2A bound to each other in A172 cells (Figure 6H). We also assessed the impact of USP15 on TOP2A ubiquitination. Overexpression of USP15 significantly reduced the endogenous ubiquitination of TOP2A in A172 cells. Accordingly, in the presence or absence of MG132, silencing endogenous USP15 promoted TOP2A ubiquitination (Figures 6I and 6J). Moreover, overexpression of USP15 markedly reduced K48-linked ubiquitination, but not K63-linked ubiquitination (Figures 6K and 6L). Therefore, USP15 interacts with TOP2A and prevents its K48-linked ubiquitination. The above findings showed that TOP2A regulation by GINS1 was dependent on USP15-mediated deubiquitination in glioma cells. In addition, USP15 overexpression reversed the inhibitory effects of GINS1 silencing on proliferation and migration ability of in U251 cells, whereas USP15 knockdown impaired the stimulatory effects of GINS1 overexpression on proliferation and migration ability of A172 cells (Figures 6M–6P). Consistently, USP15 shRNA impaired the protein levels of MMP9, N-cadherin, and Vimentin, but recovered E-cadherin expression in GINS1-overexpressing A172 cells, while the USP15 plasmid restored the protein levels of MMP9, N-cadherin, and Vimentin, but attenuated E-cadherin expression in GINS1-silenced U251 cells (Figure 6Q). Overall, these results revealed that GINS1 promotes glioma cell proliferation and migration by USP15-mediated deubiquitination of TOP2A.

Both TOP2A and USP15 are upregulated in glioma and correlated with poor prognosis

The above data revealed that TOP2A and USP15 led to the oncogenicity of GINS1. Thus, the expression and correlation of TOP2A and USP15 in clinical glioma specimens were examined. The expression levels of TOP2A and USP15 were markedly higher in glioma tissues than in the corresponding adjacent normal brain tissues. They showed a close correlation, as determined by IHC staining, Western blotting, and RT-PCR analysis (Figures 7A–7D). The GEPIA database also indicated that the expression levels of TOP2A and USP15 were higher in glioma tissues than in normal brain tissues (Figures S4A and S4B). Furthermore, the TCGA and CGGA survival data from Kaplan–Meier Plots revealed that patients with glioma with high TOP2A or USP15 expression had poorer overall survival (OS) rate, progression-free survival (PFS) rate, and disease-free survival (DFS) rate than patients with glioma with low TOP2A or USP15 expression (Figures 7E–7J and S4C–S4H). These observations suggested that higher TOP2A and USP15 expression reflected a poor glioma prognosis. In conclusion, TOP2A and USP15 were upregulated in glioma, and a good correlation predicted poor prognosis, reinforcing our proposal that GINS1 promotes glioma cell proliferation and migration by USP15-mediated TOP2A deubiquitination.

DISCUSSION

GINS1 mainly acts as a DNA replication-relevant factor that has been implicated in the progression of multiple types of tumors. This study explored whether GINS1 was upregulated in glioma cells and specimens. High expression of GINS1 predicted an advanced clinical grade and poor survival probability. Subsequent loss-of-function and gain-of-function experiments *in vitro* and *in vivo* showed that GINS1 significantly promoted cancer cell proliferation and migration, indicating the carcinogenic role of GINS1 in regulating glioma progression. Consistent with these results, recent studies have revealed that GINS1 serves as an oncogene to induce breast cancer, colorectal cancer, and hepatocellular carcinoma (Toda et al., 2020; Bu et al., 2020; Li et al., 2021). Notably, the underlying mechanism by which GINS1 functions as a glioma proliferation and migration promoter is to physically interact with TOP2A, while USP15 directly deubiquitinates TOP2A.

TOP2A is an enzyme that controls and alters DNA topologic states. TOP2A plays a crucial role in proliferation, metastasis, tumor recurrence, and metabolism and it is strictly controlled at the transcriptional, translational, and posttranslational levels (Albadine et al., 2009; Chen et al., 2013). In response to cellular stress, TOP2A protein levels change rapidly, primarily dependent on protein stability regulation (Shvero et al., 2008). Enhanced TOP2A expression was found in several cancers, including glioma (Albadine et al., 2009; Schindlbeck et al., 2010; Shvero et al., 2008; Song et al., 2018; Deguchi et al., 2017). In our study, we found that TOP2A mRNA and protein levels were upregulated in glioma tissues compared to those in adjacent normal brain tissues, that higher TOP2A expression reflected a poor glioma prognosis and that TOP2A overexpression promoted cell proliferation and migration. Importantly, the key findings of this study showed that GINS1 physically interacts with TOP2A, while GINS1 induces glioma cell proliferation and migration in a TOP2A-dependent manner. GINS1 overexpression significantly increased TOP2A protein levels to promote glioma cell proliferation and migration. Although GINS1 did not function as a deubiquitinase to impede TOP2A ubiquitination, we identified USP15 as the deubiquitinase that interacted with and directly deubiquitinated TOP2A.

USP15 belongs to a subfamily of deubiquitinases and is a widely expressed deubiquitinase that has been implicated in diverse cellular processes in cancer (Reyes-Turcu et al., 2009). USP15 has been shown to deubiquitinate receptor-activated SMADs and TRIM25 and antagonize Parkin-mediated mitochondrial ubiquitination, and USP15 regulates the TGF-β pathway and is a key factor in glioblastoma pathogenesis (Eichhorn et al., 2012; Pauli et al., 2014; Inui et al., 2011). Ubiquitination is an important cellular mechanism for targeted degradation of proteins, which is instrumental for various cellular processes, including but not limited to, transcription, cell proliferation progression, programmed cell death, and antigen presentation (Sun et al., 2020). Here, we identified USP15 as a deubiquitinase that interacted with and deubiquitinated TOP2A directly. Surprisingly, prior studies suggest that USP15 regulates TOP2A to maintain genome integrity, which is in agreement with our results (Fielding et al., 2018). Our data also revealed that USP15 mRNA and protein levels were upregulated in glioma tissues compared to those in adjacent normal brain tissues, that higher USP15 expression reflected a poor glioma prognosis and that USP15 overexpression promoted cell proliferation and migration. Moreover, USP15 knockdown reversed the TOP2A inhibition induced by GINS1 silencing and the upregulation of TOP2A expression induced by GINS1 overexpression. USP15 overexpression significantly reduced the endogenous ubiquitination of TOP2A, and silencing endogenous

USP15 promoted TOP2A ubiquitination. Importantly, similar to other deubiquitinases (Zhong et al., 2013), we found that USP15 deubiquitinates K48-linked TOP2A ubiquitination. In addition, USP15 overexpression reversed the inhibited proliferation and migration ability of glioma cells induced by GINS1 silencing in U251 cells, whereas USP15 knockdown impaired the elevated proliferation and migration ability of glioma cells induced by GINS1 overexpression in A72 cells. These results collectively suggest that GINS1 promotes glioma cell proliferation and migration by USP15-mediated TOP2A deubiquitination.

In summary, our integrated analyses have identified for the first time that a GINS1-USP15-TOP2A axis represents a critical mechanism in the proliferation and migration of glioma cells (Figure 8). Hence, blocking this axis may be a potent therapeutic strategy against glioma.

Limitations of the study

Although some significant discoveries were presented in this study, there are several limitations that must be mentioned. For example, we utilized subcutaneous xenograft tumor model, but not an intracranial orthotopic xenograft tumor model, to show the carcinogenic role of GINS1 in regulating glioma progression. However, no intracranial tumor xenograft model has been developed to assess the downregulation and overexpression of GINS1 in orthotopic tumorigenic properties. This limitation requires further investigation. Despite these limitations, we revealed that GINS1 promotes the proliferation and migration of glioma cells by USP15-mediated deubiquitination of TOP2A.

STAR★METHODS

Detailed methods are provided in the online version of this paper and include the following:

- KEY RESOURCES TABLE
- RESOURCE AVAILABILITY
  - Lead contact
  - Materials availability
  - Data and code availability
- EXPERIMENTAL MODEL AND SUBJECT DETAILS
  - Human tissue samples
  - Cell culture and reagents
  - Xenografted tumor model
- METHOD DETAILS
  - Cell transfection
  - Quantitative real-time polymerase chain reaction (qRT–PCR)
  - Western blotting assay and immunoprecipitation (IP) analysis
  - Immunohistochemical (IHC) staining
  - Cell proliferation assay
  - Colony formation assay
  - Cell migration and invasion assays
  - Co-immunoprecipitation and mass spectrometry
  - Glutathione S-transferase pull-down experiments
- QUANTIFICATION AND STATISTICAL ANALYSIS

SUPPLEMENTAL INFORMATION

Supplemental information can be found online at https://doi.org/10.1016/j.isci.2022.104952.

ACKNOWLEDGMENTS

This work was supported by the National Natural Science Foundation of China (NO. 81802503, 81772180, 82072370, and 81972213), Key University Science Research Project of Anhui Province (NO. KJ2020A0607), Fudan University Shanghai Cancer Center for Outstanding Youth Scholars Foundation (NO. YJYQ201803), Funding of "Climbing Peak" Training Program for Innovative Technology team of Yijishan Hospital, Wannan Medical College (PF201904), and Funding of "Peak" Training Program for Scientific Research of Yijishan Hospital, Wannan Medical College (GF2019T01 and GF2019G15). We thank our colleague, Dr. Shizhang Ling, for editing the language of our manuscript during the revision of this manuscript.

AUTHOR CONTRIBUTIONS

K.L., M.M., and H.Y. designed the study. H.Y. wrote the paper. X.L., X.Z., Y.W., and M.Zh. performed the cellular, molecular experiments. H.Y. performed the other all experiments and analyzed the data. M.Zh. contributed reagents/materials and animal housekeeping. All authors approved the final version of the manuscript.

DECLARATION OF INTERESTS

The authors declare that they have no competing interests.

Received: October 8, 2021
Revised: May 27, 2022
Accepted: August 12, 2022
Published: September 16, 2022

REFERENCES

Albadine, R., Wang, W., Brownlee, N.A., Toubaji, A., Billis, A., Argani, P., Epstein, J.I., Garvin, A.J., Cousi, R., Schaeffer, E.M., et al. (2009). Topoisomerase II alpha status in renal medullary carcinoma: immuno-expression and gene copy alterations of a potential target of therapy. J. Urol. *182*, 735–740.

Alchanati, I., Teicher, C., Cohen, G., Shemesh, V., Barr, H.M., Nakache, P., Ben-Avraham, D., Idelevich, A., Angel, I., Livnah, N., et al. (2009). The E3 ubiquitin-ligase Bmi1/Ring1A controls the proteasomal degradation of Top2alpha cleavage complex - a potentially new drug target. PLoS One *4*, e8104.

Bu, F., Zhu, X., Zhu, J., Liu, Z., Wu, T., Luo, C., Lin, K., and Huang, J. (2020). Bioinformatics analysis identifies a novel role of GINS1 gene in colorectal cancer. Cancer Manag. Res. *12*, 11677–11687.

Chang, Y.P., Wang, G., Bermudez, V., Hurwitz, J., and Chen, X.S. (2007). Crystal structure of the GINS complex and functional insights into its role in DNA replication. Proc. Natl. Acad. Sci. USA *104*, 12685–12690.

Chen, S.H., Chan, N.L., and Hsieh, T.S. (2013). New mechanistic and functional insights into DNA topoisomerases. Annu. Rev. Biochem. *82*, 139–170.

Chen, T., Sun, Y., Ji, P., Kopetz, S., and Zhang, W. (2015). Topoisomerase IIα in chromosome instability and personalized cancer therapy. Oncogene *34*, 4019–4031.

Chen, Z.J., and Sun, L.J. (2009). Nonproteolytic functions of ubiquitin in cell signaling. Mol. Cell *33*, 275–286.

Cuya, S.M., Bjornsti, M.A., and van Waardenburg, R.C.A.M. (2017). DNA topoisomerase-targeting chemotherapeutics: what's new? Cancer Chemother. Cancer Chemother. Pharmacol. *80*, 1–14.

Deguchi, S., Katsushima, K., Hatanaka, A., Shinjo, K., Ohka, F., Wakabayashi, T., Zong, H., Natsume, A., and Kondo, Y. (2017). Oncogenic effects of evolutionarily conserved noncoding RNA ECONEXIN on gliomagenesis. Oncogene *36*, 4629–4640.

Eguren, M., Álvarez-Fernández, M., García, F., López-Contreras, A.J., Fujimitsu, K., Yaguchi, H., Luque-García, J.L., Fernández-Capetillo, O., Muñoz, J., Yamano, H., and Malumbres, M. (2014). A synthetic lethal interaction between APC/C and topoisomerase poisons uncovered by proteomic screens. Cell Rep. *6*, 670–683.

Eichhorn, P.J.A., Rodón, L., Gonzàlez-Juncà, A., Dirac, A., Gili, M., Martínez-Sáez, E., Aura, C., Barba, I., Peg, V., Prat, A., et al. (2012). USP15 stabilizes TGF-β receptor I and promotes oncogenesis through the activation of TGF-β signaling in glioblastoma. Nat. Med. *18*, 429–435.

Fielding, A.B., Concannon, M., Darling, S., Rusilowicz-Jones, E.V., Sacco, J.J., Prior, I.A., Clague, M.J., Urbé, S., and Coulson, J.M. (2018). The deubiquitylase USP15 regulates topoisomerase II alpha to maintain genome integrity. Oncogene *37*, 2326–2342.

Gambus, A., Jones, R.C., Sanchez-Diaz, A., Kanemaki, M., van Deursen, F., Edmondson, R.D., and Labib, K. (2006). GINS maintains association of Cdc45 with MCM in replisome progression complexes at eukaryotic DNA replication forks. Nat. Cell. Biol. *8*, 358–366.

Hershko, A., and Ciechanover, A. (1998). The ubiquitin system. Annu. Rev. Biochem. *67*, 425–479.

Hou, G., Deng, J., You, X., Chen, J., Jiang, Y., Qian, T., Bi, Y., Song, B., Xu, Y., and Yang, X. (2020). Mining topoisomerase isoforms in gastric cancer. Gene *754*, 144859.

Inui, M., Manfrin, A., Mamidi, A., Martello, G., Morsut, L., Soligo, S., Enzo, E., Moro, S., Polo, S., Dupont, S., et al. (2011). USP15 is a deubiquitylating enzyme for receptor-activated SMADs. Nat. Cell Biol. *13*, 1368–1375.

Kanemaki, M., Sanchez-Diaz, A., Gambus, A., and Labib, K. (2003). Functional proteomic identification of DNA replication proteins by induced proteolysis in vivo. Nature *423*, 720–724.

Kimura, T., Cui, D., Kawano, H., Yoshitomi-Sakamoto, C., Takakura, N., and Ikeda, E. (2019). Induced expression of GINS complex is an essential step for reactivation of quiescent stem-like tumor cells within the peri-necrotic niche in human glioblastoma. J. Cancer Res. Clin. Oncol. *145*, 363–371.

Kristensen, B.W., Priesterbach-Ackley, L.P., Petersen, J.K., and Wesseling, P. (2019). Molecular pathology of tumors of the central nervous system. Ann. Oncol. *30*, 1265–1278.

Li, S., Wu, L., Zhang, H., Liu, X., Wang, Z., Dong, B., and Cao, G. (2021). GINS1 induced sorafenib resistance by promoting cancer stem properties in human hepatocellular cancer cells. Front. Cell Dev. Biol. *9*, 711894.

Li, W., Bengtson, M.H., Ulbrich, A., Matsuda, A., Reddy, V.A., Orth, A., Chanda, S.K., Batalov, S., and Joazeiro, C.A.P. (2008). Genome-wide and functional annotation of human E3 ubiquitin ligases identifies MULAN, a mitochondrial E3 that regulates the organelle's dynamics and signaling. PLoS One *3*, e1487.

Liu, X., Zhang, M., Zhu, X., Wang, Y., Lv, K., and Yang, H. (2021). Loss of FAM60A attenuates cell proliferation in glioma via suppression of PI3K/Akt/mTOR signaling pathways. Transl. Oncol. *14*, 101196.

Lou, Z., Minter-Dykhouse, K., and Chen, J. (2005). BRCA1 participates in DNA decatenation. Nat. Struct. Mol. Biol. *12*, 589–593.

Louis, D.N., Perry, A., Reifenberger, G., von Deimling, A., Figarella-Branger, D., Cavenee, W.K., Ohgaki, H., Wiestler, O.D., Kleihues, P., and Ellison, D.W. (2016). The 2016 world Health organization classification of tumors of the central nervous system: a summary. Acta Neuropathol. *131*, 803–820.

Mevissen, T.E.T., and Komander, D. (2017). Mechanisms of deubiquitinase specificity and regulation. Annu. Rev. Biochem. *86*, 159–192.

Miller, K.D., Ostrom, Q.T., Kruchko, C., Patil, N., Tihan, T., Cioffi, G., Fuchs, H.E., Waite, K.A., Jemal, A., Siegel, R.L., and Barnholtz-Sloan, J.S. (2021). Brain and other central nervous system tumor statistics, 2021. CA. CA. Cancer J. Clin. *71*, 381–406.

Nakopoulou, L., Zervas, A., Lazaris, A.C., Constantinides, C., Stravodimos, C., Davaris, P., and Dimopoulos, C. (2001). Predictive value of topoisomerase II alpha immunostaining in urothelial bladder carcinoma. J. Clin. Pathol. *54*, 309–313.

Nitiss, J.L. (2009). DNA topoisomerase II and its growing repertoire of biological functions. Nat. Rev. Cancer *9*, 327–337.

Pauli, E.K., Chan, Y.K., Davis, M.E., Gableske, S., Wang, M.K., Feister, K.F., and Gack, M.U. (2014). The ubiquitin-specific protease USP15 promotes RIG-I-mediated antiviral signaling by deubiquitylating TRIM25. Sci. Signal. *7*, ra3.

Reyes-Turcu, F.E., Ventii, K.H., and Wilkinson, K.D. (2009). Regulation and cellular roles of ubiquitin-specific deubiquitinating enzymes. Annu. Rev. Biochem. *78*, 363–397.

Schindlbeck, C., Mayr, D., Olivier, C., Rack, B., Engelstaedter, V., Jueckstock, J., Jenderek, C., Andergassen, U., Jeschke, U., and Friese, K. (2010). Topoisomerase IIalpha expression rather than gene amplification predicts responsiveness of adjuvant anthracycline-based chemotherapy in women with primary breast cancer. J. Cancer Res. Clin. Oncol. *136*, 1029–1037.

Shamaa, A.A., Zyada, M.M., Wagner, M., Awad, S.S., Osman, M.M., and Abdel Azeem, A.A. (2008). The significance of Epstein Barr virus (EBV) & DNA topoisomerase II alpha (DNA-Topo II alpha) immunoreactivity in normal oral mucosa, oral epithelial dysplasia (OED) and oral squamous cell carcinoma (OSCC). Diagn. Pathol. *3*, 45.

Shinagawa, H., Miki, Y., and Yoshida, K. (2008). BRCA1-mediated ubiquitination inhibits topoisomerase II alpha activity in response to oxidative stress. Antioxid. Redox Signal. *10*, 939–949.

Shvero, J., Koren, R., Shvili, I., Yaniv, E., Sadov, R., and Hadar, T. (2008). Expression of human DNA Topoisomerase II-alpha in squamous cell carcinoma of the larynx and its correlation with clinicopathologic variables. Am. J. Clin. Pathol. *130*, 934–939.

Siegel, R.L., Miller, K.D., Fuchs, H.E., and Jemal, A. (2021). Cancer statistics, 2021. CA. CA. Cancer J. Clin. *71*, 7–33.

Silantyev, A.S., Falzone, L., Libra, M., Gurina, O.I., Kardashova, K.S., Nikolouzakis, T.K., Nosyrev, A.E., Sutton, C.W., Mitsias, P.D., and Tsatsakis, A. (2019). Current and future trends on diagnosis and prognosis of glioblastoma: from molecular biology to proteomics. Cells *8*, 863.

Song, J., Ma, Q., Hu, M., Qian, D., Wang, B., and He, N. (2018). The inhibition of miR-144-3p on cell proliferation and metastasis by targeting TOP2A in HCMV-positive glioblastoma cells. Molecules *23*, 3259.

Sun, T., Liu, Z., and Yang, Q. (2020). The role of ubiquitination and deubiquitination in cancer metabolism. Mol. Cancer *19*, 146.

Toda, H., Seki, N., Kurozumi, S., Shinden, Y., Yamada, Y., Nohata, N., Moriya, S., Idichi, T., Maemura, K., Fujii, T., et al. (2020). RNA-sequence-based microRNA expression signature in breast cancer: tumor-suppressive miR-101-5p regulates molecular pathogenesis. Mol. Oncol. *14*, 426–446.

Vos, S.M., Tretter, E.M., Schmidt, B.H., and Berger, J.M. (2011). All tangled up: how cells direct, manage and exploit topoisomerase function. Nat. Rev. Mol. Cell. Biol. *12*, 827–841.

Vos, R.M., Altreuter, J., White, E.A., and Howley, P.M. (2009). The ubiquitin-specific peptidase USP15 regulates human papillomavirus type 16 E6 protein stability. J. Virol. *83*, 8885–8892.

Wang, J.C. (2002). Cellular roles of DNA topoisomerases: a molecular perspective. Nat. Rev. Mol. Cell Biol. *3*, 430–440.

Wen, P.Y., Weller, M., Lee, E.Q., Alexander, B.M., Barnholtz-Sloan, J.S., Barthel, F.P., Batchelor, T.T., Bindra, R.S., Chang, S.M., Chiocca, E.A., et al. (2020). Glioblastoma in adults: a Society for Neuro-Oncology (SNO) and European Society of Neuro-Oncology (EANO) consensus review on current management and future directions. Neuro Oncol. *22*, 1073–1113.

Yang, H., Liu, X., Zhu, X., Li, X., Jiang, L., Zhong, M., Zhang, M., Chen, T., Ma, M., Liang, X., and Lv, K. (2021). CPVL promotes glioma progression via STAT1 pathway inhibition through interactions with the BTK/p300 axis. JCI Insight *6*, e146362.

Zhong, B., Liu, X., Wang, X., Liu, X., Li, H., Darnay, B.G., Lin, X., Sun, S.C., and Dong, C. (2013). Ubiquitin-specific protease 25 regulates TLR4-dependent innate immune responses through deubiquitination of the adaptor protein TRAF3. Sci. Signal. *6*, ra35.

Zou, Q., Jin, J., Hu, H., Li, H.S., Romano, S., Xiao, Y., Nakaya, M., Zhou, X., Cheng, X., Yang, P., et al. (2014). USP15 stabilizes MDM2 to mediate cancer-cell survival and inhibit antitumor T cell responses. Nat. Immunol. *15*, 562–570.

STAR★METHODS

KEY RESOURCES TABLE

REAGENT or RESOURCE	SOURCE	IDENTIFIER
Antibodies		
Anti-GINS1/PSF1	Abcam	Cat#ab183524; RRID:AB_2922402
Anti-TOP2A	Abcam	Cat#ab12318; RRID:AB_299006
Anti-USP15	Abcam	Cat#ab71713; RRID: AB_2304348
Anti-USP15	Abcam	Cat#ab97533; RRID: AB_10678830
Anti-PRPF8	Abcam	Cat#ab24550; RRID: AB_448137
Anti-VCP	Abcam	Cat#ab109240; RRID:AB_10862588
Anti-EBP1	Abcam	Cat#ab180602; RRID:AB_2922403
Anti-TOP2A	Cell Signaling Technology	Cat#12286; RRID: AB_2797871
Anti-MMP9	Cell Signaling Technology	Cat#13667; RRID: AB_2798289
Anti-E-cadherin	Cell Signaling Technology	Cat#14472; RRID: AB_2728770
Anti-N-cadherin	Cell Signaling Technology	Cat#13116; RRID: AB_2687616
Anti-Vimentin	Cell Signaling Technology	Cat#5741; RRID: AB_10695459
Anti-Bcl-2	Cell Signaling Technology	Cat#15071; RRID: AB_2744528
Anti-Bcl-xl	Cell Signaling Technology	Cat#2764; RRID: AB_2228008
Anti-BAX	Cell Signaling Technology	Cat#5023; RRID: AB_10557411
Anti-Myc-Tag	Cell Signaling Technology	Cat#2276; RRID: AB_331783
Anti-Flag	Cell Signaling Technology	Cat#14793; RRID: AB_2572291
Anti-Ubiquitin	Cell Signaling Technology	Cat#3936; RRID: AB_331292
Anti-NPM	Cell Signaling Technology	Cat#3542; RRID: AB_2155178
Anti-Ki67	Cell Signaling Technology	Cat#9449; RRID: AB_2797703
Anti-GINS1	Invitrogen	Cat#PA5-50621; RRID:AB_2636074
Anti-β-Actin	Sigma-Aldrich	Cat#A1978; RRID: AB_476692
Anti-rabbit IgG, HRP-linked Antibody	Cell Signaling Technology	Cat#7074; RRID: AB_2099233
Anti-mouse IgG, HRP-linked Antibody	Cell Signaling Technology	Cat#7076; RRID: AB_330924
Chemicals, peptides, and recombinant proteins		
DMEM	Invitrogen	Cat#11965092
FBS	Gibco	Cat#12664025C
PBS	Gibco	Cat# 14190144
0.25%Trypsin-EDTA	Gibco	Cat#25200056
Cycloheximide	Selleck Chemicals	Cat# S7418
MG132	Selleck Chemicals	Cat# S2619
chloroquine diphosphate	Selleck Chemicals	Cat# S4157
GINS1 knockdown	GeneChem	N/A
TOP2A knockdown	GeneChem	N/A
USP15 knockdown	GeneChem	N/A
GINS1 plasmid	GeneChem	N/A
TOP2A plasmid	GeneChem	N/A
USP15 plasmid	GeneChem	N/A
Trizol	Invitrogen	Cat#15596018
RIPA lysis buffer	Beyotime	Cat#P0013C
SDS–PAGE	Beyotime	Cat#P0014A
0.22-μm nitrocellulose membrane	Pall	Cat#S80209

(*Continued on next page*)

Continued

REAGENT or RESOURCE	SOURCE	IDENTIFIER
Non-fat milk	Beyotime	Cat#P0216-300g
TBS	Beyotime	Cat#P0228
Tween 20	Beyotime	Cat#ST825-100mL
Chemiluminescent ECL Plus reagents	Millipore	Cat#WBKLS0500
crystal violet	Beyotime	Cat#C0121-500mL
Critical commercial assays		
SYBR Green PCR kit	ThermoFisher	Cat#4309155
ImmunoPure Metal enhanced DAB substrate kit	ThermoFisher	Cat#34065
The Pierce™ Classic Magnetic IP/Co-IP Kit	ThermoFisher	Cat#88804
MTT assay kit	Beyotime	Cat#C0009S
BCA assay kit	Beyotime	Cat#P0012
Experimental models: Cell lines		
HEB cell line	ATCC	N/A
T98G cell line	ATCC	N/A
U251 cell line	ATCC	N/A
U373 cell line	ATCC	N/A
A172 cell line	ATCC	N/A
Experimental models: Organisms/strains		
BALB/c nude mice	SIMM, CAS	N/A
Oligonucleotides		
GINS1 primers:	Sangon Biotech	N/A
F:5′-AAAGTCAGGTGGACGAAG-3′		
R:5′-CATTTGGCAAGACGCTAC-3′		
TOP2A primers:	Sangon Biotech	N/A
F:5′-CACCTAAGCTGCACAGTTCC-3′		
R: 5′-GGCTGCCTCCTAATTCTTCC-3′		
USP15 primers:	Sangon Biotech	N/A
F:5′-TGCCTACTTCCAACTCTC-3′		
R:5′-GCTCTTCCTTTCCTTCTC-3′		
GAPDH primers:	Sangon Biotech	N/A
F:5′-CCAGGTGGTCTCCTCTGA-3′		
R:5′-GCTGTAGCCAAATCGTTGT-3′		
Software and algorithms		
ImageJ	National Institutes of Health	https://imagej.nih.gov/ij/
SPSS 19.0	SPSS	http://www.spss.com.cn
Graphpad prime 8.0	Graphpad	https://www.graphpad.com/
Adobe Illustrator CS6	Adobe	https://www.adobe.com/products/illustrator/
Other		
CGGA - the Chinese Glioma Genome Atlas	Beijing Tiantan Hospital, Capital Medical University	http://www.cgga.org.cn/index.jsp
TCGA - the Cancer Genome Atlas	HOME for Researchers	https://www.aclbi.com/static/index.html#/tcga

(*Continued on next page*)

Continued

REAGENT or RESOURCE	SOURCE	IDENTIFIER
NCBI	National Center for Biotechnology Information	https://www.ncbi.nlm.nih.gov
GEO - Gene Expression Omnibus	National Center for Biotechnology Information	https://www.ncbi.nlm.nih.gov/geo/ GEO: GSE209547; GEO: GSE188256

RESOURCE AVAILABILITY

Lead contact

Further information and requests for resources and reagents should be directed to and will be fulfilled by the lead contact, Kun Lv (lvkun315@126.com).

Materials availability

This study did not generate new unique reagents.

Data and code availability

This paper analyzes existing, publicly available data. The accession number and link are listed in the key resources table. This paper does not report original code. Any additional information required to reanalyze the data reported in this paper is available from the lead contact upon request.

EXPERIMENTAL MODEL AND SUBJECT DETAILS

Human tissue samples

173 pairs of adjacent nontumor tissues and glioma samples were collected from the Department of Neurosurgery of the First Affiliated Hospital, Wannan Medical College (Wuhu, Anhui, P. R. China) from February 2008 to October 2011. According to the WHO guidelines, two pathologists evaluated all specimens. All tissues obtained at the surgery were directly preserved in liquid nitrogen. Patients received no systemic treatment before the surgery. Patient consent was obtained. All surveys and experiments were approved by the Ethic Committee for Clinical Research of the First Affiliated Hospital of Wannan Medical College. The clinical information of the samples is summarized in Table S5.

Cell culture and reagents

Human normal glial cell and glioma cell lines were obtained from the Cell Bank of the Chinese Academy of Sciences (Shanghai, China). The cell lines were characterized by DNA fingerprinting, cell vitality detection, isozyme detection, and mycoplasma detection. The last cell characterization was performed in December 2020. The five cell lines were cultured in high-glucose Dulbecco's modified Eagle medium (DMEM; Invitrogen, Carlsbad, CA, USA) supplemented with 10% fetal bovine serum (FBS; Gibco, Bethesda, MD, USA) and pen/strep antibiotics. All cells were incubated in 5% CO_2 at 37°C. Cycloheximide, proteasome inhibitor MG132, and chloroquine diphosphate were purchased from Selleck Chemicals (Houston, TX, USA).

Xenografted tumor model

The xenografted tumor model experimental protocol was approved by the Wannan Medical College Animal Experimental Ethics Committee. Five-week-old BALB/c nude mice (male/female ratio 1:1) were obtained from the Shanghai Institute of Materia Medica, Chinese Academy of Science and maintained under specific pathogen-free conditions. For the tumorigenesis assay, 6×10^6 cells (U251-shGINS1 cells, U251-shCtrl cells, A172-GINS1 cDNA cells and A172-pcDNA3.1 cells) in 200 μL of PBS were implanted subcutaneously into the right dorsal flank of the mice (4 mice for each group). All mice were sacrificed 4 weeks after inoculation. Tumor volume was calculated with the following formula: Volume = 0.5 × length × width^2.

METHOD DETAILS

Cell transfection

The lentivirus constructs of GINS1 knockdown, TOP2A knockdown, USP15 knockdown, GINS1 plasmid, TOP2A plasmid and USP15 plasmid were obtained from GeneChem (Shanghai, China). Glioma cell lines

were plated in 6-well microplates at 50% confluence and infected with lentivirus-mediated knockdown shRNA or scrambled control shRNA in U251 and T98G cells, respectively. For plasmid transfection, A172 cells were seeded in 6-well microplates and transfected with control vector plasmid or GINSI cDNA, TOP2A cDNA, or USP15 cDNA when the cell density reached 70–80% confluence. The above cell transfection protocol was based on the manufacturer's instructions. Stable transduction pools were generated by puromycin selection for two weeks. The cells were cultured after transfection and harvested for the following experiments.

Quantitative real-time polymerase chain reaction (qRT–PCR)

With TRIzol reagent, total RNA was extracted from cells or tissues. According to the manufacturer's instructions, the qRT–PCR assay was performed using the SYBR Green PCR kit. Relative expression levels were calculated by the $2^{-\Delta\Delta CT}$ method. Each sample was repeated in triplicate and analyzed using relative quantification method.

Western blotting assay and immunoprecipitation (IP) analysis

The proteins from cells or tissues, the protein concentration, and the 10% SDS–PAGE isolated protein were extracted with RIPA lysis buffer, measured with a BCA assay kit, and transferred to a 0.22-μm nitrocellulose membrane. The membranes were blocked at room temperature with 5% non-fat milk for 2 h. Then, each membrane was incubated with one of the indicated specific primary antibodies. The membranes were washed with 0.1% TBST three times for 5 min and then incubated with anti-mouse or anti-rabbit IgG HRP-linked secondary antibody for 2 h. Each was washed with 0.1% TBST three times for 5 min. Chemiluminescent ECL Plus reagents were added to visualize the reaction products. The membranes, the band intensity, and the protein levels were scanned with Tanon 5200, measured by densitometry using Quantity One Software, and normalized to that of β-actin. All experiments were repeated independently thrice, and representative results are shown.

Immunohistochemical (IHC) staining

Paraffin-embedded mouse tumor tissues was cut into 5-μm-thick section for the IHC analysis of GINS1, TOP2A and USP15 protein. After baking for 2 h at 60°C, the tissues were immersed in xylene for deparaffinization and rehydrated with a series of ethanol at decreased concentrations. Then, the tissue sections were incubated with the following one of primary antibodies for 12 h at 4°C. The tissue sections were washed with PBS and incubated with biotinylated secondary antibody for 2 h at room temperature the next day. Finally, tissue sections were treated with an ImmunoPure Metal enhanced DAB substrate kit in accordance with the manufacturers' instructions.

Cell proliferation assay

Cell proliferation assays were performed with MTT assays according to the manufacturer's instructions. In brief, 2×10^3 glioma cells from each group were collected and inoculated into 96-well microplates. Then, the cells were incubated with 50 μL MTT solution for 3 h. At 490 nM, the absorbance value of each well was measured by a microplate reader. Six replicates were set up in each group, and then the mean value was taken.

Colony formation assay

Glioma cells were plated in 6-well microplates and cultured in the appropriate culture medium for 2 weeks. The culture medium was changed every 3 days. Cell colonies were stained with 1% crystal violet and then counted.

Cell migration and invasion assays

Transwell assays and wound healing assays were used to measure the migration and invasion of glioma cells. For transwell assays, glioma cells in each group were inoculated into the upper chamber of the Transwell chamber (BD Biosciences, USA) at the density of 4×10^4 cells/well. Besides, 500 μL culture medium containing 10% fetal bovine serum was added to the 24-well culture plate of the lower chamber. After 24 h of routine culture, the chamber was removed, and cells from the upper layer of microporous membranes were wiped with cotton swabs. After that, cells were immobilized in 4% paraformaldehyde solution for 10 min at room temperature and stained with 0.5% crystal violet solution (Sigma-Aldrich; Merck KGaA) for 15 min. In the last step, 5 visual fields were randomly selected and observed under an optical microscope (Nikon,

Japan) to count the number of cells invading the sub-layer of the microporous membranes of the chamber. For wound healing assays, when the transfected glioma cells were maintained in a 6-well plate, achieving 90-95% confluence, scratches were generated using the micropipette tips. The wound state was observed at 0 and 72 h after scratching with an X71 inverted microscope (Olympus, Tokyo, Japan) (Liu et al., 2021; Yang et al., 2021).

Co-immunoprecipitation and mass spectrometry

The Pierce Classic Magnetic IP/Co-IP Kit was used to examine proteins bound to GINS1. Cells (1×10^7) were washed in PBS twice, and then 500 μL IP lysis buffer was added to lyse cells. One-tenth of the supernatant was saved as the input. To the remaining supernatant, 5 μg FLAG antibody-magnetic bead complex was added, and then samples were incubated at 4°C overnight. Magnetic beads were washed five times with buffer containing 10 μg/mL RNAse A before being eluted with 100 μL elution buffer. Protein samples (20 μL) were boiled in LDS buffer for Western blotting, and 80 μL protein samples were analyzed by label-free LC/MS.

Glutathione S-transferase pull-down experiments

Glutathione S-transferase fusion constructs were expressed in *Escherichia coli* BL21 cells, and crude bacterial lysates were prepared by sonication in cold PBS in the presence of a protease inhibitor mixture. *In vitro* transcription and translation experiments were performed with rabbit reticulocyte lysate. In GST pull-down assays, ~10 μg of the appropriate GST fusion protein was mixed with 5–8 μL of the *in vitro* transcribed/translated products and incubated in binding buffer. The binding reaction was then added to 30 μL of glutathione Sepharose beads and mixed at 4°C for 2 h. The beads were washed five times with binding buffer, resuspended in 30 μL of 2× SDS–PAGE loading buffer, and resolved on 12% gels. Protein bands were detected with specific antibodies by Western blotting.

QUANTIFICATION AND STATISTICAL ANALYSIS

All data from three independent experiments are expressed as the mean ± SD, and statistical analyses were performed using SPSS 19.0 software. Student's *t* test was used to examine the differences between the two groups, and ANOVA was used to investigate the differences in multiple groups. The chi-square test was applied to examine the relationship between GINS1 levels and clinicopathological characteristics. Overall survival, progression-free survival and disease-free survival rates were analyzed using the Kaplan–Meier plot and tested via the log rank test. Statistics were regarded as significant when *, $p < 0.05$.